DEUTSCHES ELEKTRONEN-SYNCHROTRON DESY

DESY 88-003
January 1988

RADIATIVE CORRECTIONS TO HIGH ENERGY PROCESSES AND PRECISION TESTS OF THE ELECTROWEAK THEORY

by

W. Hollik

II. Institut für Theoretische Physik, Universität Hamburg

ISSN 0418-9833

NOTKESTRASSE 85 · 2 HAMBURG 52

To be sure that your preprints are promptly included in the
HIGH ENERGY PHYSICS INDEX ,
send them to the following address (if possible by air mail) :

DESY
Bibliothek
Notkestrasse 85
2 Hamburg 52
Germany

DESY 88-003
January 1988

ISSN 0418-9833

Radiative Corrections to High Energy Processes and Precision Tests of the Electroweak Theory

WOLFGANG HOLLIK
II. INSTITUT FÜR THEORETISCHE PHYSIK
UNIVERSITÄT HAMBURG, FRG

Abstract

Precision tests of the electroweak theory in future experiments at the e^+e^- colliders LEP and SLC are discussed at the level of radiative corrections. The influence of the electroweak radiative corrections on the theoretical predictions for the vector boson masses M_W, M_Z, the on-resonance e^+e^- asymmetries, and for the Z resonance shape are reviewed for the Standard Model and for its extension by a second Higgs doublet.

Lectures given at the "11th International School of Theoretical Physics", Szczyrk, Poland, September 1987

1 Introduction.

The structure of the electroweak Standard Model as a spontaneously broken gauge theory implies that the theoretical prediction of any observable quantity can be calculated to an arbitrary order of perturbation theory in terms of a given set of input parameters. For an adequate analysis of the high precision experiments feasible at the e^+e^- colliders LEP and SLC /1,2/ the inclusion of radiative corrections becomes indispensible:

- High precision experiments can test the validity of radiative corrections and therefore test the Standard Model at the quantum level. Their verification would be a milestone in establishing the Standard Model as a quantized field theory.
- Possible "new physics" will probably manifest in terms of small deviations from the Standard Model predictions which have therefore to be known with high accuracy. New heavy particles may contribute through radiative corrections to the relations between the electroweak measurable quantities.
- Radiative corrections can be large, in particular the bremsstrahlung corrections around the Z resonance. Their proper treatment in the data analysis is of basic importance for testing the non-QED part of the electroweak theory.

Electroweak processes between fermions can be described by essentially three parameters, e.g. the SU(2) and U(1) coupling constants g_2 and g_1, and v, the vacuum expectation value of the Higgs field. Equivalently, another set can be used where every parameter represents a typical experiment at low momentum transfer:

- the fine structure constant $\alpha = 1/137.03604$, obtained from Thomson scattering;
- the Fermi constant $G_\mu = 1.16637 \times 10^{-5}\ GeV^{-2}$, obtained from the μ lifetime;
- the mixing angle $\sin^2\theta_W$, obtained from neutrino scattering.

The relations between these quantities and the masses of the vector bosons M_W,M_Z, as derived from the minimal model in lowest order

$$1 - M_W^2/M_Z^2 = \sin^2\theta_W$$

$$M_W^2 \sin^2\theta_W = \pi\alpha/\sqrt{2}G_\mu$$

are in general modified by the inclusion of radiative corrections, depending on the details of a chosen renormalization scheme. This will be discussed in Section 2. Moreover, the determination of the fermionic couplings to the Z

$$v_f = \frac{I_f^3 - 2Q_f \sin^2\theta_W}{2\sin\theta_W\cos\theta_W}$$

$$a_f = \frac{I_f^3}{2\sin\theta_W\cos\theta_W}$$

from e^+e^- data give experimental information in addition to α and G_μ. In Sections 3 and 4 we discuss the response of the theoretical e^+e^- cross sections and asymmetries to the presence of radiative corrections.

2 Parameters and renormalization.

The Standard model has a certain number of free parameters which are not fixed by the theory. The definition of these parameters and their relation to measureable quantities is the duty of a renormalization scheme, which completes the definition of the quantized theory.

The favoured renormalization scheme in QED is the on-shell scheme with the fermion masses m_f and the fine structure constant (the on-shell e-e-γ coupling) as input parameters. The most direct and natural extension extension to the electroweak theory leads to the on-shell (OS) scheme of SU(2)×U(1) /3-6/, which has been widely used for practical applications (see e.g ref's /1,2/). Differences in the treatment of field renormalization and in the unphysical sector should disappear in the final relations between physical quantities. Here we follow the OS scheme as specified in /5/.

Starting point is the classical Lagrangian

$$L_{cl} = L_G(W, B, g_2, g_1) + L_H(\phi, \mu^2, \lambda) + L_{FG}(\psi_L, \psi_R, W, B) + L_{FH}(\psi_L, \psi_R, \phi, g_f) \qquad (2.1)$$

L_G is the gauge part with the SU(2) and U(1) fields W and B and the corresponding gauge couplings g_2, g_1; L_H is the Higgs part with the scalar doublet ϕ and the potential parameters μ^2, λ; L_{FG} describes the fermion–gauge field interaction with left and right handed fermion fields $\psi_{L,R}$, and L_{FH} is the Higgs-fermion Yukawa term that induces the fermion masses.

In the fields and parameters of (2.1) the SU(2)×U(1) symmetry of L_{cl} is manifestly apparent. The physical content, however, becomes more transparent after switching to the "physical" fields and parameters

$$W^{\pm}, Z, \gamma;\ e, M_W, M_Z, m_f. \qquad (2.2)$$

There is no room for $\sin^2\theta_W$ as an additional independent quantity. The simplest choice in terms of (2.2) that makes the Z-γ mixing in (2.1) vanish is

$$\sin^2\theta_W = 1 - M_W^2/M_Z^2 \qquad (2.3)$$

which will be used throughout the forthcoming discussion.

Since it is convenient to work in a renormalizable gauge (t'Hooft-Feynman gauge) the gauge fixing term L_{fix} and the corresponding Fadeev-Popov ghost term L_{gh} have to be added to L_{cl} in order to obtain the Lagrangian for the quantized theory. Multiplicative field and parameter renormalization introduces renormalization constants $\sqrt{Z_2^i}$ for each field multiplet and Z_1^i for each free parameter in the original manifest symmetric version. These renormalization constants are then determined by the renormalization conditions.

The renormalization conditions give the parameters in (2.2) the physical meaning which we expect them to have. The first class are the OS conditions for the 2-point functions which make the particle content of the theory evident:

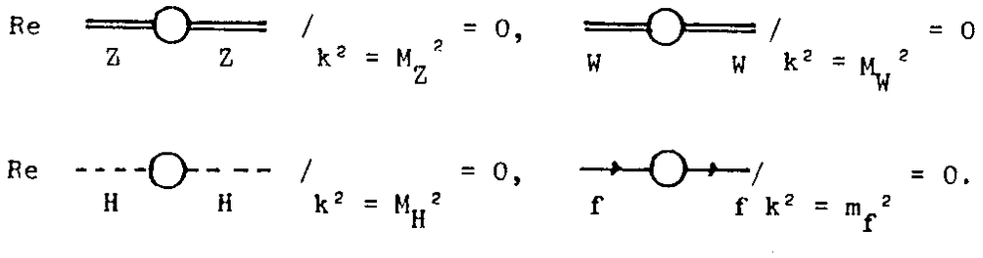

(2.4)

(The bubbles mean the one-loop contributions together with the counter terms.)

The second class defines the electric charge in the Thomson limit and allows to recover the ordinary QED as a simple substructure:

(2.5)

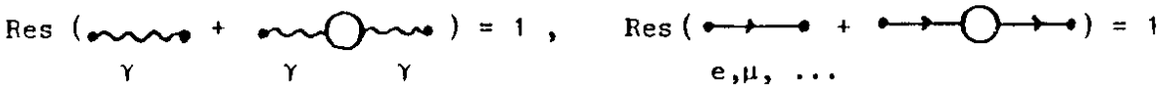

The results can be summarized in terms of renormalized self energies Σ^j in the propagators (where $j = \gamma$,Z,W)

$$\frac{1}{q^2 - M_j^2 + iM_j\Gamma_j} \longrightarrow \frac{1}{q^2 - M_j^2 + \Sigma^j(q^2)} \tag{2.6}$$

the mixing energy $\Sigma^{\gamma Z}(q^2)$, and the vector and axialvector formfactors $F_{V,A}^{jf}(q^2)$ for the Zff, γff and Wff' vertices. A complete list can be found in /5/.

The advantages of the OS scheme are obvious:

- The input parameters have a clear physical meaning and can be measured directly.
- Except the Higgs and top mass M_H, m_t all parameters are known.
- It has a natural separation into "QED corrections" (virtual and real bremsstrahlung) and infrared finite "weak corrections". This is of practical importance for the implementation into Monte Carlo programs.

The W mass M_W is not known as precisely as to make the uncertainty in the radiative corrections negligible (ΔM_W = 100 MeV with LEP200). This drawback can easily be overcome by including the OS radiative correction to the μ lifetime in eq. (1.2) /3/:

$$M_W^2(1 - M_W^2/M_Z^2) = \frac{\pi\alpha}{\sqrt{2}G_\mu} \frac{1}{1 - \Delta r(\alpha, M_W, M_Z, M_H, m_t)} \tag{2.7}$$

As done in /5,7/the non-QED correction Δr can be written in terms of the renormalized W self energy Σ^W (which depends on all particle masses of the model) and the sum of vertex, box, and wave function renormalization contributions:

$$\Delta r = \frac{\Sigma^W(0)}{M_W^2} + \frac{\alpha}{4\pi \sin^2\theta_W}(6 + \frac{7 - 4\sin^2\theta_W}{2\sin^2\theta_W}\log(\cos^2\theta_W)) \tag{2.8}$$

The reward of (2.7) is twofold:

- It is interesting by itself since it allows a comparison of the M_W - M_Z - $\sin^2\theta_W$ correlation with the experimental data.
- It provides a value for M_W (after specifying the other masses) as well as for $\sin^2\theta_W$, which can be used as numerical input for the calculation of other observables of interest. These parameter values are given in Table 1 for various Z, Higgs, and top masses.

The hadronic QED-type contribution to Δr can be evaluated with help of a dispersion integral over the measured cross section for $e^+e^- \rightarrow$ hadrons /8/. The analysis of Jegerlehner /9/ leads to the result (for 5 flavors, $M_Z = 93$ GeV):

$$\Delta r^{(5)}_{had,QED} = 0.0286 \pm 0.0007$$

This value has been used as input for Table 1. Other recent determinations of Δr_{had} /10/ give a larger error $\delta(\Delta r) = 0.0013$. A further source of uncertainty is the scheme dependence /11/ yielding an additional $\delta(\Delta r) = 0.0011$.

The variation of $\sin^2\theta_W$ with M_H (from 1 GeV to 1 TeV) of 0.005 matches the present experimental uncertainty of $\Delta \sin^2\theta_W = \pm 0.005$ from neutrino nucleon scattering The strong dependence on a large top mass can be utilized to derive an upper limit on m_t from the experimental values of M_W, M_Z /12/: $m_t \lesssim 185$ GeV (1σ). Including the information from neutral current neutrino data this limit can be improved /13/ : $m_t \lesssim 200$ GeV at 90% confidence level.

Table 1: W mass and $\sin^2\theta_W = sw$ from eq.(2.7). All masses in GeV.

		MH=10		MH=100		MH=1000 GEV	
MZ	MT	SW	MW	SW	MW	SW	MW
90.	50.	0.2429	78.31	0.2445	78.23	0.2477	78.06
90.	100.	0.2376	78.59	0.2392	78.50	0.2425	78.33
90.	150.	0.2316	78.89	0.2333	78.81	0.2366	78.63
90.	200.	0.2239	79.29	0.2256	79.20	0.2291	79.02
90.	230.	0.2181	79.58	0.2199	79.49	0.2235	79.31
91.	50.	0.2354	79.57	0.2370	79.49	0.2401	79.33
91.	100.	0.2301	79.85	0.2317	79.77	0.2349	79.60
91.	150.	0.2241	80.16	0.2257	80.07	0.2290	79.90
91.	200.	0.2164	80.56	0.2181	80.47	0.2215	80.29
91.	230.	0.2106	80.85	0.2123	80.76	0.2158	80.58
92.	50.	0.2283	80.82	0.2298	80.74	0.2329	80.58
92.	100.	0.2230	81.09	0.2246	81.01	0.2277	80.85
92.	150.	0.2170	81.41	0.2186	81.33	0.2218	81.16
92.	200.	0.2093	81.81	0.2109	81.72	0.2143	81.55
92.	230.	0.2035	82.11	0.2052	82.02	0.2086	81.84
93.	50.	0.2216	82.05	0.2231	81.97	0.2261	81.81
93.	100.	0.2164	82.33	0.2179	82.25	0.2210	82.08
93.	150.	0.2103	82.65	0.2119	82.56	0.2150	82.40
93.	200.	0.2025	83.05	0.2042	82.97	0.2075	82.79
93.	230.	0.1967	83.35	0.1984	83.27	0.2018	83.09
94.	50.	0.2153	83.27	0.2167	83.19	0.2197	83.03
94.	100.	0.2101	83.55	0.2116	83.47	0.2146	83.30
94.	150.	0.2039	83.87	0.2055	83.79	0.2086	83.62
94.	200.	0.1962	84.28	0.1978	84.19	0.2010	84.02
94.	230.	0.1903	84.58	0.1920	84.50	0.1953	84.32
95.	50.	0.2092	84.48	0.2107	84.40	0.2136	84.24
95.	100.	0.2041	84.75	0.2056	84.67	0.2086	84.51
95.	150.	0.1979	85.08	0.1994	85.00	0.2025	84.84
95.	200.	0.1901	85.49	0.1917	85.41	0.1949	85.24
95.	230.	0.1842	85.80	0.1859	85.72	0.1892	85.54

3 High energy e^+e^- processes.

3.1 $e^+e^- \longrightarrow \mu^+\mu^-$

The two Born diagrams

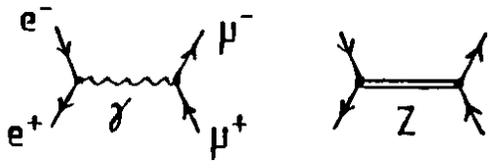

yield the differential cross section in lowest order for polarized electron beams (P_L : degree of longitudinal e^- polarization)

$$\frac{d\sigma}{d\Omega} = \frac{\alpha^2}{4s}(\sigma_u - P_L\sigma_{pol}) \tag{3.1}$$

with $s = (p_{e-} + p_{e+})^2$ and

$$\sigma_u = (1 + 2v_e^2 Re(\chi) + (v_e^2 + a_e^2)^2|\chi|^2)(1 + \cos^2\theta) + (2a_e^2 Re(\chi) + 4v_e^2 a_e^2|\chi|^2)\,2\cos\theta$$

$$\sigma_{pol} = 2v_e a_e(Re(\chi) + (v_e^2 + a_e^2)|\chi|^2)(1 + \cos\theta)^2 \tag{3.2}$$

and

$$\chi = s/(s - M_Z^2 + iM_Z\Gamma_Z), \qquad \theta = \sphericalangle\,(e^-, \mu^-)\,.$$

The one-loop corrections to (3.1) can be classified in the following way:

- The QED corrections to the photon exchange graph. Also the QED part of the photon vacuum polarization is included, although there is no common consensus on that.
- The QED corrections to the Z exchange graph (full QED corrections depicted in Figure 1)
- Weak corrections consisting of the propagator and vertex corrections mentioned in Section 2 and box diagrams with ZZ and WW exchange.

The QED corrections /14-16/ include the emission of bremsstrahlung quanta which have to be integrated over their allowed phase space to give an inclusive 2-particle cross section:

$$\frac{d\sigma_B}{d\Omega_\mu} = \int dk_\gamma^0\, d\Omega_\gamma\, \frac{d^5\sigma}{d\Omega_\mu\, d\Omega_\gamma\, dk_\gamma^0}$$

Adding to $d\sigma_B$ the virtual photon corrections yields an infrared finite result. Instead of the IR singularity the details of the γ phase space enter the result. Conventionally an acollinearity cut to the outgoing $\mu^+\mu^-$ momenta and/or an energy cut to the emitted photon is applied:

$$\sphericalangle\,(\mu^-, \mu^+) < \delta_{max}, \quad k_\gamma^0 < \Delta E$$

This type of corrections therefore depends on the details of the experiments and is conveniently treated by Monte Carlo simulation /15/. The weak corrections /17-21/ are independent of experimental cuts; they include the more subtle parts of the theory beyond the tree level.

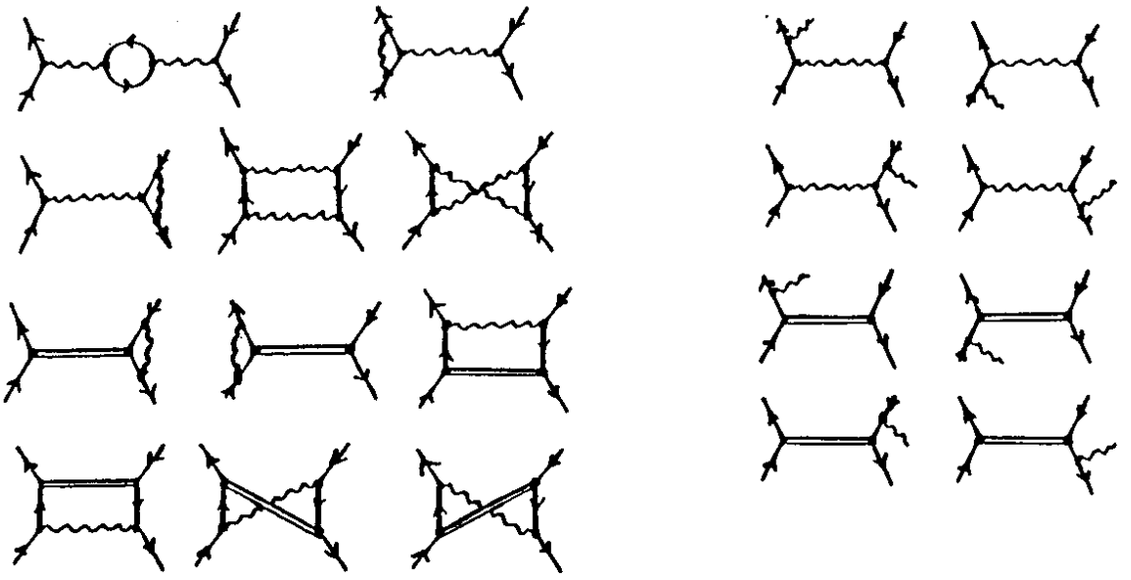

Figure 1: Full QED corrections to $e^+e^- \longrightarrow \mu^+\mu^-$

The observables of particular interest for precision electroweak tests are the on-resonance ($s = M_Z^2$) asymmetries:
- the forward-backward asymmetry

$$A_{FB} = \frac{\sigma^{for} - \sigma^{back}}{\sigma^{for} - \sigma^{back}} \tag{3.3}$$

with

$$\sigma^{for} = \int_{\theta<\pi/2} d\Omega \, \frac{d\sigma}{d\Omega}, \quad \sigma^{back} = \int_{\theta>\pi/2} d\Omega \, \frac{d\sigma}{d\Omega}$$

- the left-right asymmetry (or polarization asymmetry)

$$A_{LR} = \frac{\sigma_L - \sigma_R}{\sigma_L + \sigma_R} \tag{3.4}$$

where $\sigma_{L,R}$ denotes the integrated cross sections with left and right handed electrons. In lowest order the on-resonance asymmetries read:

$$A_{FB} \cong \frac{3}{4} \frac{4v_e^2 a_e^2}{(v_e^2 + a_e^2)^2}$$

$$A_{LR} \cong \frac{2v_e a_e}{v_e^2 + a_e^2}$$

Another interesting quantity is the polarized forward-backward asymmetry in quark pair production $e^+e^- \longrightarrow$ qq /22/

$$A_{FB}^{pol} = \frac{\sigma_L^{for} - \sigma_L^{back} - (\sigma_R^{for} - \sigma_R^{back})}{\sigma_L^{for} + \sigma_L^{back} + \sigma_R^{for} + \sigma_R^{back}} \tag{3.5}$$

which allows a direct measurement of the final state coupling constants. In lowest order this asymmetry reads on resonance:

$$A_{FB}^{pol} \cong \frac{3}{2} \frac{v_q a_q}{v_q^2 + a_q^2}$$

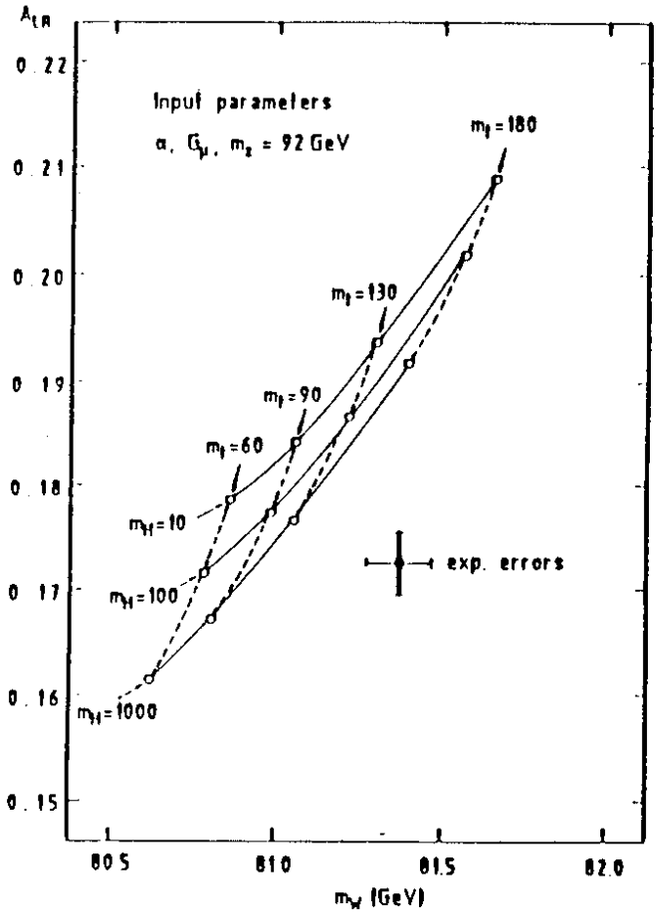

Figure 3 (from ref 2)

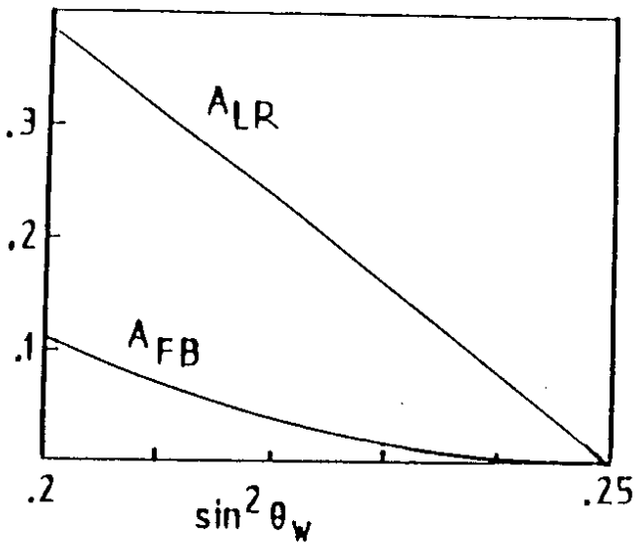

Figure 2:
Dependence of the on-resonance asymmetries on $\sin^2\theta_W$

For given M_Z both A_{FB} and A_{LR} depend on $\sin^2\theta_W$ as displayed in Figure 2. The particular sensitivity of A_{LR} to $\sin^2\theta_W$ will allow a measurement of this quantity with an error of 0.0004 if an accuracy $\Delta A_{LR} = 0.003$ is achieved /23/ (from μ, τ, quark final states together). Together with the determination of M_Z ($\Delta M_Z = 20 - 50$ MeV /1,2/) and the relation $\sin^2\theta_W$-M_Z, eq. (2.7), this will provide the most stringent precision test of the electroweak theory.

Eliminating $\sin^2\theta_W$ by means of (2.7) leads to the prediction (for fixed M_Z)

$$M_Z,\ G_\mu,\ \alpha \longrightarrow M_W(M_H, m_t),\ A_{LR}(M_H, m_t)$$

The curves for fixed m_t (dashed lines) and for fixed M_H (full lines) are shown in Figure 3. The weak corrections coming from the top and the Higgs, and the expected experimental errors make it possible to delimit the allowed mass ranges significantly. Effects of new physics (heavy quark/lepton doublets, SUSY sfermions,...) in the M_W–A_{LR} correlation have also been studied /24/; for their experimental investigation, however, the knowledge of the top mass would become a necessity.

3.2 Bhabha scattering $e^+e^- \longrightarrow e^+e^-$

The process of Bhabha scattering is of prime importance in e^+e^- collisions since it serves as a reference process for luminosity measurements and for clean tests of the electroweak theory.

The full $O(\alpha)$ electroweak corrections consisting of the QED corrections (all graphs of Figure 1 also in the t-channel), s- and t-channel propagator and vertex corrections as outlined in Section 2, and finite ZZ, WW box diagrams, have recently been calculated and put into a Monte Carlo generator /25/ (see also /26/). Parts of the radiative corrections have also been discussed in earlier work /27/.

Figure 4 contains the integrated Bhabha cross section for both final e^+, e^- within the designed angular range (θ_{min}, $180^o - \theta_{min}$) and no cuts applied to the radiated photon. The bulk of the radiative corrections comes from QED. For small angles the continuum like structure of the corrections (everywhere positive) dominates; at larger angles the typical resonance behaviour: large negative corrections at the peak, large positive corrections (radiative tail) above, becomes more and more striking. The weak corrections at $s = M_Z^2$ are only 1 - 2% .

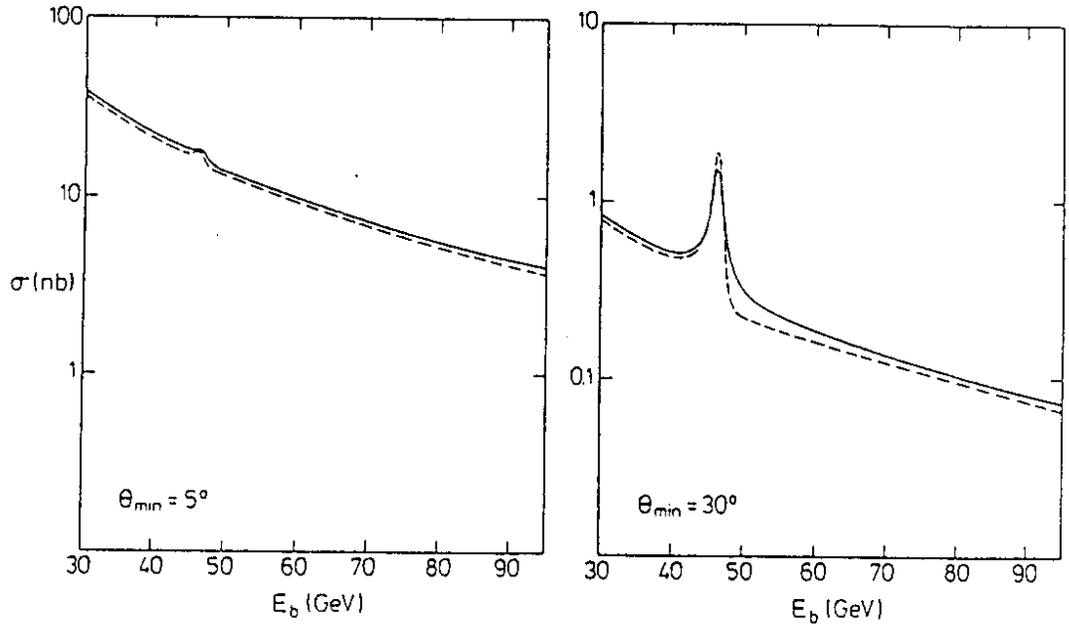

Figure 4 : Integrated Bhabha cross section as function of $E_b = \sqrt{s}/2$.
- - - - lowest order
——— $O(\alpha)$ corrected

3.3 Higher order QED corrections around the Z resonance

Since the O(α) QED corrections are large around the Z peak (typically -40%) a careful study of the next order contributions becomes necessary for precision experiments like measurements of the mass and width of the Z boson. The main source for large negative corrections is the initial state bremsstrahlung where both soft and hard photons lead to a reduction of the peak cross section: soft photons because of the absence of the ideal elastic process, and hard photons because of the energy loss in the resonance propagator. The reduction of the peak height is roughly given by the factor

$$1 - \frac{2\alpha}{\pi} \log(\frac{M_Z}{\Gamma_Z}) \log(\frac{M_Z^2}{m_e^2}) = 0.6$$

A partial summation of multiple photon emission consists of exponentiation of the infrared parts /14/ or of the leading log terms /28/:

$$1 - \frac{2\alpha}{\pi} \log(\frac{M_Z}{\Gamma_Z}) \log(\frac{M_Z^2}{m_e^2}) \quad \longrightarrow \quad \left(\frac{M_Z}{\Gamma_Z}\right)^{-\frac{2\alpha}{\pi}\log(M_Z^2/m_e^2)}$$

An exact treatment of the $O(\alpha^2)$ initial state QED corrections to the integrated $e^+e^- \longrightarrow \mu^+\mu^-$ cross section has been performed in /29/. This allows to study the shift in the resonance peak which is crucial for the Z mass measurement (Figure 5): the shift of +184 MeV from O(α) is reduced by -88 MeV due to the $O(\alpha^2)$ contributions. The remaining uncertainty is estimated from

$$O(\alpha^2)\ \textit{exponentiated} - O(\alpha^2)\ \textit{non exponentiated}$$

to be 15 MeV.

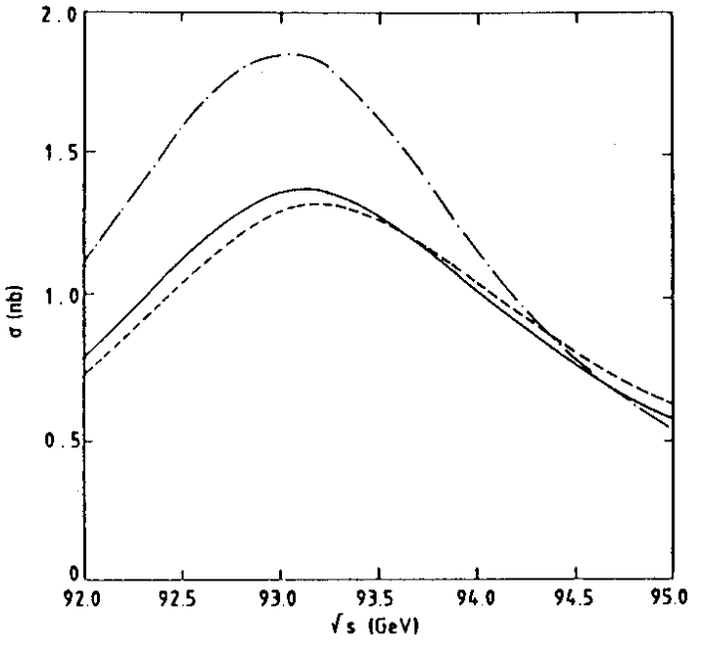

Figure 5 : Total cross section for $e^+e- \longrightarrow \mu^+\mu^-$ (from ref 29).
— · — · — Born approximation
– – – – – – O(α) corrected
———— O(α^2) corrected

A combination of this higher order initial state radiation with the weak corrections to the boson propagators including next order contributions to the Z width /30, 31/ yields the theoretical prediction for the resonance shape which has the accuracy required for measurements of the Z boson's mass and width. Some results from /30/ are listed in Table 2.

TABLE 2 : Maxima and half-maxima of the Z-resonance shape in muon-pair production for various values of M_H and m_t. M_Z=92GeV, α_s=0.12

m_t	M_H	sigmax (nb)	√s(max) (GeV)	√s(max/2,-) (GeV)	√s(max/2,+) (GeV)
40	100	1.39	92.094	90.713	93.774
60	100	1.47	92.094	90.755	93.723
90	10	1.48	92.095	90.754	93.726
90	100	1.48	92.095	90.753	93.728
90	1000	1.47	92.094	90.756	93.722
200	100	1.52	92.097	90.741	93.751

In general, the QED corrections to to e^+e^- processes constitute an obstacle in the physics analysis of high precision experiments since they are sensitive to the detector acceptances, to cuts (acollinearity, γ energy,...), and to higher order contributions. Moreover, the present status of the higher order QED corrections is not yet adequate for an accurate analysis of e.g. charge asymmetries in $e^+e^- \longrightarrow f\bar{f}$.

The on-resonance left-right asymmetry, however, is practically free of the specific QED problems because of its very small QED corrections /16,32/. The high sensitivity of A_{LR} to $\sin^2\theta_W$ makes it a unique tool for testing the internal structure of the Standard Model and to search for effects of "new physics" beyond the minimal model.

4 Radiative corrections with two Higgs doublets

4.1 General features of 2-doublet models

As an example for new physics effects in radiative corrections we consider the minimal extension of the Standard Model, which has two Higgs doublets in SU(2)×U(1) leaving the relation

$$\rho = \frac{M_W^2}{M_Z^2 \cos^2\theta_W} = 1$$

unchanged. The strongest motivation for extending the Higgs sector may come from supersymmetry. But also non-supersymmetric arguments advocate two Higgs doublets, such as the Peccei-Quinn mechanism to solve the strong CP problem /33/, and the discussion of CP violation.

The vacuum expectation values v_1, v_2 of the complex doublets ($j = 1, 2$)

$$\Phi_j = \begin{pmatrix} \phi_j^+(x) \\ (v_j + \eta_j(x) + i\,\chi_j(x))/\sqrt{2} \end{pmatrix} \qquad (4.1)$$

induce the masses of the vectorbosons in the following way:

$$M_W = \frac{1}{2} g_2 \sqrt{v_1^2 + v_2^2}, \quad M_Z = \frac{1}{2}\sqrt{g_1^2 + g_2^2}\,\sqrt{v_1^2 + v_2^2} \qquad (4.2)$$

3 of the eight degrees of freedoms of the doublet fields are absorbed in forming the longitudinal polarization states of the $W^\pm$, Z, and 5 remain as physical particles: a pair of charged Higgs bosons $\phi^\pm$, two neutral scalars H_0, H_1, and a single neutral pseudoscalar H_2. These physical states are obtained by diagonalizing the mass matrix coming from the Higgs potential:

$$\begin{aligned} \phi^+ &= -\phi_1^+ \sin\beta + \phi_2^+ \cos\beta \\ H_2 &= -\chi_1 \sin\beta + \chi_2 \cos\beta \end{aligned} \qquad (4.3a)$$

for the charged Higgs and the neutral pseudoscalar, and

$$\begin{aligned} H_0 &= \eta_1 \cos\alpha + \eta_2 \sin\alpha \\ H_1 &= -\eta_1 \sin\alpha + \eta_2 \cos\alpha \end{aligned} \qquad (4.3b)$$

for the 2 neutral scalars. The mixing angle β is determined by the v_1, v_2 :

$$\tan\beta = v_1/v_2 \qquad (4.4)$$

whereas α depends on all parameters of the Higgs potential.

In a non-SUSY 2-Higgs model the angles α,β and all the physical masses M_0, M_1 M_2 M_{ϕ^+} are independent parameters. In the minimal supersymmetric model these quantities are severely constraint /35/ :

$$\begin{aligned} M_{\phi^+}^2 &= M_W^2 + M_2^2 \\ M_{0,1}^2 &= \frac{1}{2}\left(M_Z^2 + M_2^2 \pm \sqrt{(M_Z^2 + M_2^2)^2 - 4\,M_Z^2 M_2^2 \cos^2 2\beta}\right) \\ \tan(2\alpha) &= \tan(2\beta)\,\frac{M_2^2 + M_Z^2}{M_2^2 - M_Z^2} \end{aligned} \qquad (4.5)$$

In such a model one of the neutral scalars is always lighter than the Z, whereas $M_{\phi^+} > M_W$. From present e^+e^- experiments an experimental lower bound $M_{\phi^+} > 18$ GeV was derived /36/.

If the masses of the Higgs bosons are of the weak boson mass scale or heavier there is little chance to produce them directly in the e^+e^- colliders of the next future. Indirect effects, however, may be present in the radiative corrections to the M_W-M_Z correlation and in $e^+e^- \longrightarrow f\bar{f}$ around the Z resonance.

4.2 The vector boson masses

For the calculation of radiative corrections to fermionic processes we need as additional input parameters only the Higgs masses and the mixing angles α, β. The renormalization can be performed in the OS scheme in analogy to the strategy in the minimal model based on the renormalization conditions (2.4) and (2,5). For details see ref. 38.

Application to the μ lifetime yields the analogous relation between M_W and M_Z /37,38/

$$M_W^2(1 - M_W^2/M_Z^2) = \frac{\pi\alpha}{\sqrt{2}G_\mu} \frac{1}{1 - (\Delta r + \Delta\bar{r})} \tag{4.6}$$

where the minimal radiative correction Δr is augmented by the non-standard term

$$\Delta\bar{r}(\alpha, M_W, M_Z, M_0, M_1, M_2, M_{\phi^+}; |\alpha - \beta|)$$

$\Delta\bar{r}$ depends on the two mixing angles only in the combination $|\alpha - \beta|$ as long as v_1 and v_2 do not differ by several orders of magnitude.

For general mixing in the neutral scalar sector neither H_0 nor H_1 can be identified with the "standard" Higgs. Thus, if one of them (say H_0) is included in the standard Δr it has to be subtracted in $\Delta\bar{r}$.

The numerical solution of (4.7) for the standard situation with $\Delta r(\alpha, M_W, M_Z, M_H = M_0)$, and for the 2-doublet case with

$$\Delta r + \Delta\bar{r}(\alpha, M_W, M_Z, M_0, M_1, M_2, M_{\phi^+}, \zeta)$$

yields the value for M_W after specifying M_Z and the Higgs mass(es) and $\zeta = |\alpha - \beta|$. The differences are depicted in Figure 6 as functions of the charged Higgs mass (which is assumed to be larger than M_W) for various sets of the neutral scalar/pseudoscalar masses $M_{0,1}$. The shaded area corresponds to the variation of ζ between 0 and $\pi/2$. In the case a the result is independent of ζ.

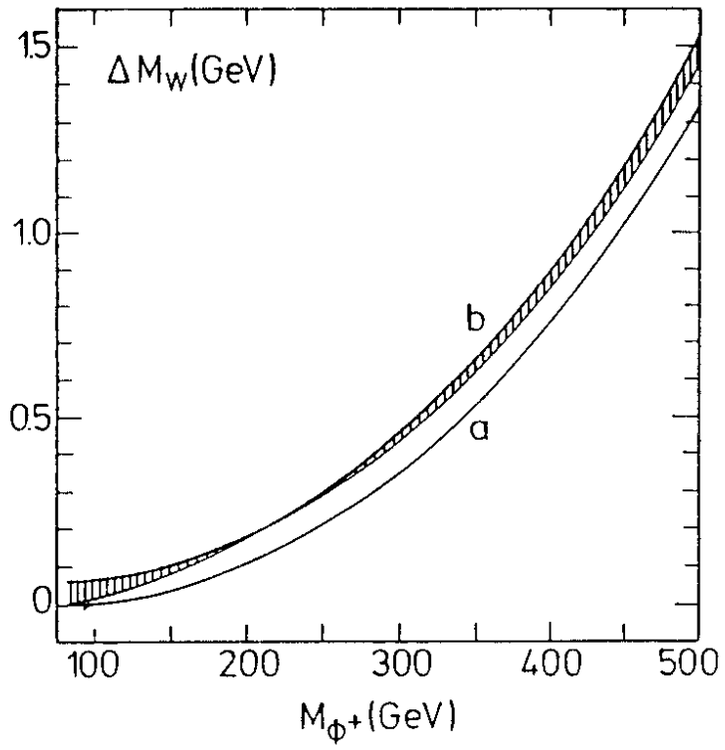

Figure 6:
Additional Higgs contributions to M_W.
$M_Z = 93$ GeV, $M_0 = M_Z$.
a) $M_1 = M_2 = M_Z$
b) $M_1 = 10$ GeV, $M_2 = M_Z$

From present M_W measurements with $\Delta M_W = 1.5$ GeV no restrictive bound on the mass splitting between the neutral and charged scalar sector can be derived. An accuracy of $\Delta M_W = 100$ MeV, as expected from LEP 200, can restrict $M_{\phi^+} < 200$ GeV if the neutral Higgs masses are $< M_Z$.

In the supersymmetric Higgs model the constraints (4.5) forbid large neutral-charged mass splittings. As a consequence, the deviations from the minimal model remain smaller than the experimental uncertainty in M_W.

4.3 Asymmetries in $e^+e^- \longrightarrow \mu^+\mu^-$

In analogy to section 3.1 we calculate the $O(\alpha)$ corrected on-resonance asymmetries A_{FB}, eq. (3.3), and A_{LR}, eq. (3.4), in the following way:

For given ζ, M_Z and Higgs masses the corresponding value for M_W resp. $\sin^2\theta_W$ is derived from (4.6). This value is used as input for the calculation of A_{FB} and A_{LR}. Then the Standard Model result (with $M_H = M_0$) is subtracted yielding the non-standard contributions. These are displayed in Figure 7 for the same set of parameters as in Figure 6. The shaded area indicates the variation with the mixing angle ζ in the neutral Higgs sector.

The left-right asymmetry shows the best sensitivity to mass splittings. An experimental accuracy of $\Delta A_{LR} = \pm 0.003$ can restrict the mass of the charged Higgs boson to $M_{\phi^+} < 160$ GeV if M_1, M_2 are of the order of the Z mass. The unpolarized forward-backward asymmetry is somewhat less restrictive: from an experimental $\Delta A_{FB} = \pm .002$ a constraint on the charged Higgs mass of $M_{\phi^+} < 200$ GeV can be obtained. This bound is comparable with that from a W mass measurement with a precision of $\Delta M_W = \pm 100$ MeV (see Figure 6).

Again, for the SUSY Higgs model with the restrictions (4.5), the absence of large mass splittings keeps the deviations from the minimal model below the experimental sensitivity.

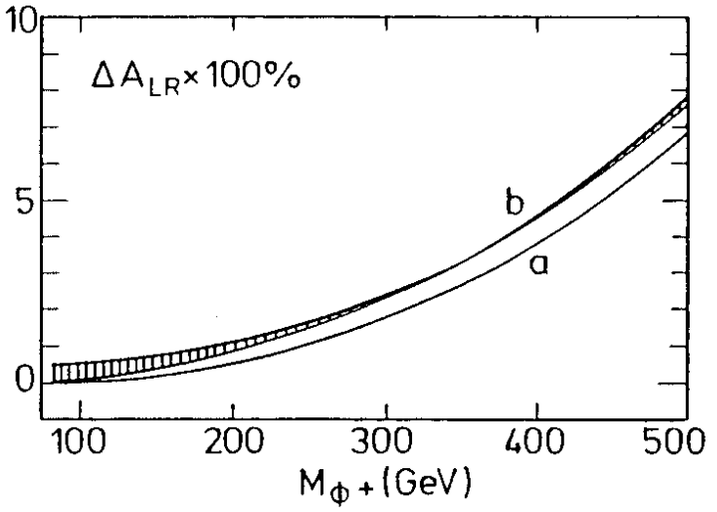

Figure 7a :
Additional Higgs Contributions to A_{LR} on-resonance
Same parameters as in Figure 6.

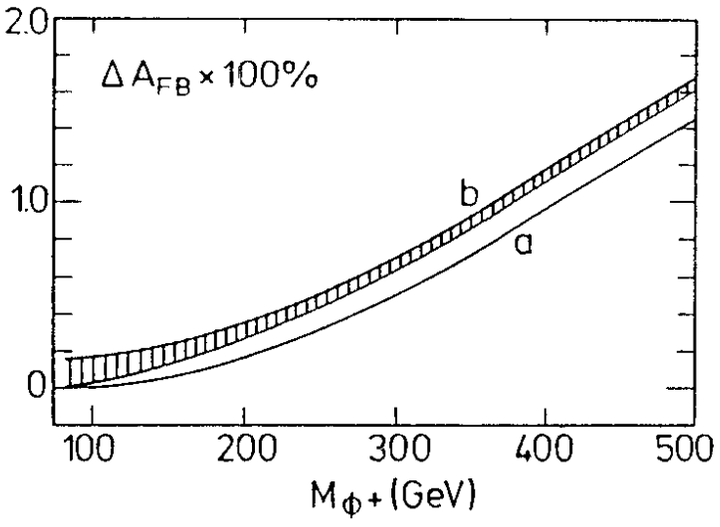

Figure 7b :
Additional Higgs Contributions to A_{FB} on-resonance
Same parameters as in Figure 6.

5 Summary

Experiments at the e^+e^- colliders LEP and SLC will determine the mass of the Z boson and the on-resonance asymmetries A_{FB} and A_{LR} with high accuracy. In connection with the precisely measured μ decay constant G_μ these experiments provide precision tests of the Standard Model after the radiative corrections have been taken into account carefully. The largest part of the radiative corrections are in general the QED corrections, which demand a treatment beyond the one-loop level. For the determination of the Z resonance shape (measurements of mass and width) and for the left-right asymmetry these corrections are under control.

Uncertainties in the radiative corrections come from the uncertainty in the hadronic contribution to the vacuum polarization and from the unknown Higgs and top mass. The error in the theoretical predictions induced by the hadronic uncertainty matches the experimental error of the future experiments. The precise measurement of M_Z, M_W and A_{LR} will restrict the allowed range of the unknown parameters M_H, m_t in the minimal model significantly.

Effects from a second Higgs doublet with large mass splitting between the charged and neutral Higgs bosons are of similar signature as the effects from a heavy top quark. In order to reveal possible signals of new physics beyond the Standard Model the knowledge of the top mass becomes a necessity.

Acknowledgement

I want to thank the organizers of the "11th International School for Theoretical Physics" for the kind hospitality and for the pleasant stay during the conference.

References

/1/ Physics with LEP, ed. J.Ellis and R. Peccei, CERN 86-02
/2/ A. Barroso et al, CERN-EP/87-70, in:
ECFA Workshop on LEP 200, ed. A.Böhm, W. Hoogland, CERN 87-08, ECFA 87-108
/3/ A. Sirlin, Phys. Rev. D 22 (1980) 971
/4/ D.A. Ross, J.C. Taylor, Nucl. Phys. B 51 (1973) 25;
S. Sakakibara, Phys. Rev. D 24 (1981) 1149;
J. Fleischer, F. Jegerlehner, Phys. Rev D 23 (1981) 2001; Nucl. Phys. B 228 (1982) 1;
K.I. Aoki et al, Suppl. Prog. Theor. Phys. 73 (1982) 1;
D.Yu. Bardin, P.Ch. Christova, O.M. Federenko, Nucl. Phys. B 175 (1980) 435; B197 (1982) 1;
/5/ M. Böhm, W. Hollik, H. Spiesberger, Fortsch. Phys. 34 (1987) 687
/6/ Radiative Corrections in SU(2)×U(1), ed. B.W. Lynn and J. Wheater, Singapore 1984
/7/ M. Böhm, W. Hollik, H. Spiesberger, Z. Phys. C 27 (1985) 523
/8/ E.A. Paschos, Nucl. Phys. B 159 (1979) 285;
W. Wetzel, Z. Phys. C 11 (1981) 117
/9/ F. Jegerlehner, Z. Phys. C 32 (1986) 195
/10/ J. Cole, G. Penso, C. Verzegnassi, Trieste Preprint 19/85/EP
/11/ F. Jegerlehner, Z. Phys. C 32 (1986) 425;
W. Hollik, H.J. Timme, Z. Phys. C 33 (1986) 125
/12/ Particle Data Group, Phys. Lett 170 B (1986) 1
/13/ U. Amaldi et al, Phys. Rev. D 36 (1987) 1385;
G. Costa et al, CERN-TH 4675/87
/14/ M.Greco, G. Pancheri, Y. Srivastava, Nucl. Phys. B 171 (1980) 118; E: B 197 (1982) 543
/15/ F.A. Berends, R. Kleiss, S. Jadach, Nucl. Phys. B 202 (1982) 63
/16/ M. Böhm, W. Hollik, Nucl. Phys. B 204 (1982) 45
/17/ W. Wetzel, Nucl. Phys. B 227 (1983) 1
/18/ M. Böhm, W. Hollik, Phys. Lett. 139 B (1984) 213
/19/ R.W. Brown, R. Decker, E.A. Paschos, Phys. Rev. Lett. 52 (1984) 1192
/20/ B.W. Lynn, R.G. Stuart, Nucl. Phys. B 253 (1985) 216
/21/ W. Hollik, Phys. Lett. 152 B (1985) 121
/22/ A. Blondel, B.W. Lynn, F.M. Renard, C. Verzegnassi, Montpellier Preprint PM/87-14 (1987)
/23/ Proposal for Polarization at the SLC, SLAC Proposal, D. Blockus et al, 1986
/24/ B.W. Lynn, M. Peskin, R.G. Stuart, in /1/
/25/ M. Böhm, A. Denner, W. Hollik, DESY 86-165;
F.A. Berends, R. Kleiss, W. Hollik, DESY 87-94
/26/ K Tobimatsu, Y. Shimizu, Prog. Theor. Phys. 75 (1986) 905
/27/ M.L.G. Readhead, Proc. Roy. Soc. 154 A (1953) 159;
Y.S. Tsai, Phys. Rev. 120 (1960) 269;
F.A. Berends, K.J.F. Gaemers, R. Gastmans, Nucl. Phys. B 68 (1974) 541;
M. Consoli, Nucl. Phys. B 160 (1979) 208;
M. Consoli, S. LoPresti, M. Greco, Phys. Lett. 113 B (1982) 415;
W. Hollik, Phys. Lett. 123 B (1983) 259;
M. Böhm, A. Denner, W. Hollik, R. Sommer, Phys. Lett. 144 B (1984) 414;
M. Greco, Phys. Lett. 177 B (1986) 97

/28/ E.A. Kuraev, V.S. Fadin, Sov. J. Nucl. Phys. 41 (1985) 446;
O. Nicrosini, L. Trentadue, Phys. Lett. 196 B (1987) 551
/29/ F.A. Berends, G.J.H. Burgers, W.L. van Neerven, Phys. Lett. 185 B (1987) 395;
CERN-TH 4772/87
/30/ F.A. Berends, G.J.H. Burgers, W. Hollik, W.L. van Neerven, CERN-TH 4919/87
/31/ W. Beenakker, W. Hollik, in preparation
/32/ S. Jadach, J.H. Kühn, R.G. Stuart, MPI-PAE/PTH 71/87
/33/ R.D. Peccei, H.R. Quinn, Phys. Rev. Lett. 38 (1977) 1440; Phys. Rev. D 16 (1977) 1719
/34/ A.J. Buras, Proc. of the EPS Conference, Bari 1985, and references therein
/35/ H.E. Haber, G.L. Kane, Phys. Rep. 117 (1985) 75;
J.F. Gunion, H.E. Haber, Nucl. Phys. B 272 (1986) 1
/36/ CELLO Collaboration, DESY 87-30
/37/ S. Bertolini, Nucl. Phys. B 272 (1986) 77
/38/ W. Hollik, Z. Phys. C 32 (1986)291;
DESY 87-68 (Z. Phys. C, to appear)